

# Shear Wave Dispersion in Lean Versus Steatotic Rat Livers

Christopher T. Barry, MD, PhD, Christopher Hazard, PhD, Zaegyoo Hah, PhD, Gang Cheng, PhD, Alexander Partin, BS, Robert A. Mooney, PhD, Kuang-Hsiang Chuang, PhD, Wenqing Cao, PhD, Deborah J. Rubens, MD, Kevin J. Parker, PhD

Received June 26, 2014, from the Departments of Surgery (C.T.B., K.-H.C.), Pathology and Laboratory Medicine (R.A.M., W.C.), and Radiology (D.J.R.), University of Rochester Medical Center, Rochester, New York USA; GE Global Research, Niskayuna, New York USA (C.H.); Department of Electrical and Computer Engineering (Z.H., A.P., K.J.P.), University of Rochester, Rochester, New York USA; and GE Global Research, Shanghai, China (G.C.). Revision requested August 25, 2014. Revised manuscript accepted for publication September 15, 2014.

This work was partially supported by GE Healthcare and the University of Rochester Center for Emerging and Innovative Sciences. Portions of the material were presented at the 2014 American Institute of Ultrasound in Medicine Annual Convention; March 31, 2014; Las Vegas, Nevada.

Address correspondence to Kevin J. Parker, PhD, Department of Electrical and Computer Engineering, University of Rochester, Hopeman Building, 203, PO Box 270126, Rochester, NY 14627-0126 USA.

E-mail kevin.parker@rochester.edu

## Abbreviations

NAFLD, nonalcoholic fatty liver disease; NASH, nonalcoholic steatohepatitis; TG, triglyceride

doi:10.7863/ultra.34.6.1123

**Objectives**—The precise measurement of fat accumulation in the liver, or steatosis, is an important clinical goal. Our previous studies in phantoms and mouse livers support the hypothesis that, starting with a normal liver, increasing accumulations of microsteatosis and macrosteatosis will increase the lossy viscoelastic properties of shear waves in a medium. This increase results in an increased dispersion (or slope) of the shear wave speed in the steatotic livers.

**Methods**—In this study, we moved to a larger animal model, lean versus obese rat livers ex vivo, and a higher-frequency imaging system to estimate the shear wave speed from crawling waves.

**Results**—The results showed elevated dispersion in the obese rats and a separation of the lean versus obese liver parameters in a 2-dimensional parameter space of the dispersion (slope) and shear wave speed at a reference frequency of 150 Hz.

**Conclusions**—We have confirmed in 3 separate studies the validity of our dispersion hypothesis in animal models.

**Key Words**—dispersion; fatty liver; medical ultrasound; shear waves; steatosis

**N**onalcoholic fatty liver disease (NAFLD) is a growing national health problem, with an estimated prevalence of 23% to 33.6%.<sup>1-4</sup> Nonalcoholic fatty liver disease is part of metabolic syndrome, which consists of 3 or more of the following: obesity, hypertension, elevated fasting blood glucose levels, hypertriglyceridemia, and low high-density lipoprotein levels. It is estimated that 2% to 3% of patients with NAFLD progress to nonalcoholic steatohepatitis (NASH) and from there to cirrhosis, liver failure, or hepatocellular carcinoma.<sup>5</sup> However, in a recent study of 400 adult volunteers (55% nonobese) enrolled in sonographic screening for steatosis with liver biopsy, the overall prevalence of NAFLD was 46%, and the prevalence of NASH was 12.2%,<sup>6</sup> suggesting that the prevalence is higher than previously estimated. Nonalcoholic fatty liver disease affects 80% of patients with metabolic syndrome, and in patients undergoing bariatric surgery, up to 96% have NAFLD, and 25% have NASH.<sup>1</sup> Nonalcoholic fatty liver disease is actually a higher risk factor for cardiovascular mortality and malignancy than for liver-related mortality.<sup>7</sup> The risk factors for NAFLD (obesity and insulin resistance/type 2 diabetes) are increasing dramatically, and the incidence of NAFLD and NASH is rising proportionately. Recent estimates indicate that the prevalence

of obesity in the United States is 33.8%.<sup>5</sup> Although standard therapy for NAFLD and NASH has been weight loss or bariatric surgery, pharmacologic agents are being developed in clinical trials.<sup>5</sup> Currently, the only quantitative measurements for steatosis are liver biopsy (which is invasive with concomitant patient risk) and magnetic resonance imaging (which is relatively expensive and not widely available). Thus, there is an urgent need for a noninvasive and readily available method to quantify hepatic fat, which is a biomarker for hepatic disease and metabolic syndrome. This study supports the scientific basis for sonographic steatosis measurement using shear wave dispersion. In concert with additional fibrosis and inflammation measurements, this approach may lead to a widely available and inexpensive method for diagnosing and monitoring NAFLD and NASH.

Currently, liver fibrosis staging can be measured by several approved magnetic resonance imaging and sonographic systems approved by the US Food and Drug Administration. In addition, transient elastography, which has no imaging component, is performed by FibroScan (Echosens, Paris, France). Studies have shown promising results for characterization of later-stage fibrosis.<sup>8–13</sup> In one study, the accuracy for measuring fibrosis approached 92% for the imaging technique versus 84% for the nonimaging technique when determining fibrosis stages 0 and 1 vs. 2 to 4 (METAVIR scoring<sup>14</sup>) in a series of 121 patients with chronic hepatitis C. Only 10% of the patients in this series had substantial steatosis (>33%), so the effect of steatosis on fibrosis measurement is unknown.<sup>15</sup> Transient elastography of fibrosis has been assessed in a series of patients selected for obesity and fatty liver disease, achieving accuracy of 84% for stages F2 and higher when using a lower insonating frequency. Discordance between sonographic and histologic findings for at least 2 stages was noted in patients with a higher body mass index and lower levels of fibrosis.<sup>16</sup> These are precisely the patients likely to have the greatest steatosis because the quantity of hepatic fat diminishes as the degree of fibrosis increases. Compared to a larger body of studies of shear wave speed and fibrosis, relatively few studies have examined the frequency-dependent shear wave properties related to dispersion or viscoelastic models.<sup>8,17–22</sup>

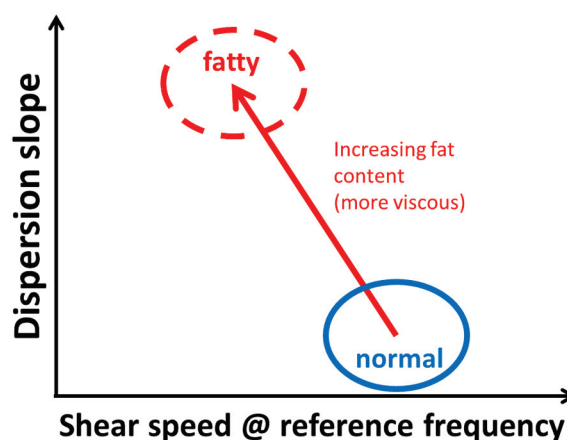
Our method builds on the principles of elastography to include measurements of dispersion (the upward slope of the shear wave speed and attenuation with frequency), which results from viscosity within the liver and consequently increases with steatosis. We apply crawling waves<sup>23</sup> to the liver over a range of shear wave frequencies between 80 and 200 Hz, and the necessary Doppler data are collected in a cine loop of less than 3 seconds. The resulting disper-

sion measurements, which vary with frequency, may help separate the effects of fibrosis (increased stiffness with little dispersion) from fat (softer and more viscous with more dispersion) and, particularly, enable differentiation of lean versus steatotic livers. Figure 1 illustrates our hypothesis. Our preliminary work<sup>24–26</sup> has demonstrated supporting evidence for this principle.

In our first (pilot) study of normal versus fatty livers in a mouse model,<sup>24</sup> we introduced the hypothesis that increasing the amount of fat in the liver would increase the dispersion of the shear wave velocity, resulting in an increase in the slope of the shear speed and shear attenuation versus frequency. This result is a consequence of adding a viscous element, triglyceride (TG), to the liver medium. We reported results from ex vivo measurements of 14 mice divided into 2 groups: lean (<5% steatosis) and obese ( $\approx 65\%$  steatosis). The dispersion or slope of the shear speed versus frequency was found to be statistically significantly different ( $P < .003$ ) between the groups. Dispersion (meters per second per 100 Hz) was low in lean mouse livers ( $0.16 \pm 0.03$ ) and higher in obese mouse livers ( $0.23 \pm 0.04$ ), as measured over a shear wave frequency band centered around 260 Hz.

In our second and expanded study,<sup>27</sup> we assessed ex vivo livers from a group of 70 mice that had progressively longer durations on a steatotic diet. The objective was to assess the progressive increase in shear wave dispersion against the progressive increase in steatosis for mice as a function of time. Group analysis of livers containing less than 0.1 mg of TG/mg of liver (“low fat”;  $n = 30$ ), 0.1 to 0.25 mg of TG/mg of liver (“moderate-high fat”;  $n = 21$ ), and greater than 0.25 mg of TG/mg of liver (“very high

**Figure 1.** Two-parameter hypothesis, considering the dispersion as an independent parameter related to viscous or lossy components.



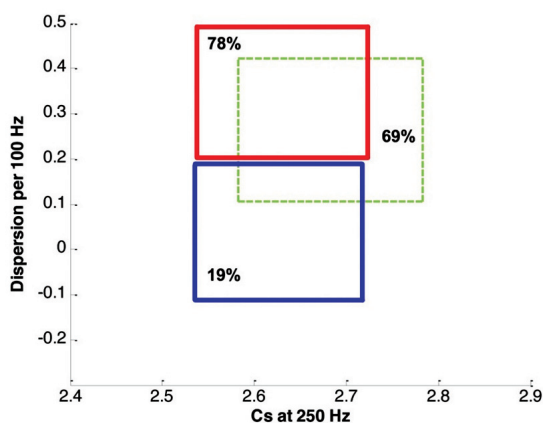
fat<sup>27</sup>; n = 17) revealed mean dispersion values of 0.05, 0.28, and 0.35 cm/s per 100 Hz, respectively. These TG groupings corresponded to visual assessments of 19%, 69%, and 78% steatosis from examination of hematoxylin-eosin-stained tissue sections.

Figure 2 demonstrates that dispersion slopes tend to increase with increasing TG levels; however, the reference shear speed at 250 Hz is relatively unchanged. We further demonstrated that the dispersion within subgroups was shown to be near 0 for normal mouse livers (steatosis <5%) and increased to 0.2 to 0.5 m/s per 100 Hz in the group with TG levels of greater than 0.25 mg/mg of liver. Thus, the possibility exists for staging progressive grades of steatosis by careful measurement of shear wave dispersion.

## Materials and Methods

In this study, we moved to a larger animal model, a higher-frequency imaging transducer, and a state-of-the-art LOGIQ E9 scanner (GE Healthcare, Wauwatosa, WI). Animal studies were performed in accordance with protocols approved by the University of Rochester's Committee on Animal Resources. Male obese Zucker-*Lepr<sup>fa/fa</sup>* and lean control Zucker-*Lepr<sup>+</sup>* rats were purchased from Harlan Research Laboratories (Indianapolis, IN) at 10 weeks of age. Rats were placed on a LabDiet (St Louis, MO) 5001 diet (13.5% fat). After a 1-week acclimation period, lean rats were used in the studies. Two weeks later, the obese rats were analyzed.

**Figure 2.** Analysis of 70 ex vivo mouse livers grouped into low fat (19% average), moderate-to-high fat (69% average), and high fat (78% average) as measured in a previous study.<sup>27</sup> The 2-dimensional parameter space shows dispersion (y-axis) versus the shear speed ( $c_s$ ) value at 250 Hz (x-axis). The boxes define the 90% confidence intervals for the linear fits of (slope, reference value) for the 3 groups.



Before scanning, rats were injected intraperitoneally with ketamine (60 mg/kg) and xylazine (4 mg/kg). Abdominal hair was removed with a depilatory, and the rat was secured in the supine position. Additional ketamine injections were given as needed to achieve a state of slow respirations for minimizing motion artifacts. After transcutaneous scanning was performed, the rats were euthanized by cervical dislocation, hepatectomy was performed, and the excised livers were placed in 9.3% gelatin for support for scanning and production of crawling waves.

After hepatectomy, two small portions of the liver were evaluated histologically and biochemically. Histologic examination of the percentage of hepatic steatosis was performed by a single experienced pathologist (W.C.) using hematoxylin-eosin-stained tissue sections.<sup>28</sup> A TG (a representative of fat concentration<sup>29</sup>) assay was performed and reported as milligrams of TG per gram of liver. The rest of the liver was suspended in a gelatin phantom for crawling wave scanning.

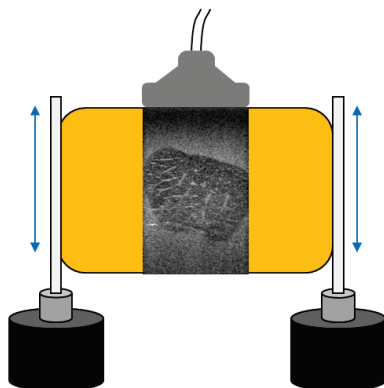
The TG extraction protocol was modified from Burant et al.<sup>30</sup> We weighed the frozen liver pieces and homogenized them in chloroform:methanol (2:1 vol/vol). Then we filtered extracts through fluted filter paper (grade 802 qualitative fluted filter papers; Whatman, Little Chalfont, England). Sulfuric acid (0.05% in saline) was added to filtered extract at a ratio of 1:5 (vol/vol). After centrifugation, the chloroform layer was removed, dried down, and resuspended in fresh chloroform. Samples were then diluted in 5% Triton X-100 (Sigma, St Louis, MO) (in chloroform) and evaporated. Finally, we measured TG in duplicate using an L-type TG kit (Wako Chemicals, Inc, Richmond, VA).

The crawling wave experimental setup used a dual-channel function generator (model AFG3022B; Tektronix, Beaverton, OR) to produce two sinusoidal signals with a slight difference of 0.35 Hz between the frequencies. The signals were passed through a power amplifier (model 5530; AE Techron, Elkhart, IN) and subsequently were supplied to piston vibration sources (model 4810; Brüel & Kjaer, Naerum, Denmark). Two elongated bars with rough surfaces of 8 × 1 cm were mounted on the pistons and placed in close contact at opposite sides of the gelatin phantom, thereby generating shear wave propagation from each side.<sup>27</sup> The 9.3% (by mass) gelatin phantom consisted of 1800 mL of degassed water, 184.5 g of gelatin, 2.7 g of agar, and 16.2 g of salt. All of the ingredients were mixed together, heated to 65°C, and then cooled to 32°C before being poured into a sample holder, where the liver was suspended on a fishing wire. The liver samples in gelatin were immediately placed in a refrigerator to cool and solidify.

When solidified, the phantom was removed from the refrigerator to reach room temperature before being scanned using the crawling wave method. Less than 24 hours was needed from liver resection to scanning time. A linear array ultrasound transducer (L8-18i-D; GE Healthcare, Wauwatosa, WI) was positioned between the vibration sources and scanned the medium. The configuration is shown in Figure 3.

A special research package was developed for the GE LOGIQ E9 system to enable crawling wave sonography. The color flow processing was modified to display only the variance of the power spectral density. Thresholds designed to improve color flow imaging were modified to support the display of variance in the tissue regions. Specially designed finite impulse response filters replaced the normal wall filters. The standard wall filters are designed to remove the tissue signals, and they complicate the relationship between the variance and the vibration amplitudes. The specially designed finite impulse response filters remove direct current contributions and allow for imaging of smaller amplitudes of vibration.<sup>31</sup> The real-time variance calculations in the GE LOGIQ E9 system were modified to match methods used in offline processing. This process allowed for an improved display of the crawling wave patterns in real time, which permitted adjustment of the experimental setup to optimize the data collection. The unprocessed quadrature data were also added to Digital Imaging and Communications in Medicine files of the saved images. Special MATLAB (The MathWorks, Natick, MA) routines were written to extract the quadrature data and allow for further offline processing. In addition, a trigger signal was provided to allow synchronization with the mechanical vibration system if desired.

**Figure 3.** Schematic of the ex vivo measurement configuration showing the shear wave sources on the right and left in contact with a gelatin phantom surrounding the liver (center). The imaging transducer is on top.



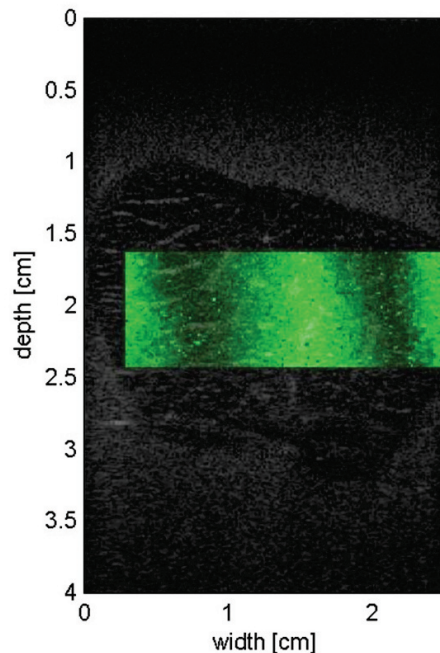
A region of interest within the liver specimen was chosen using the 18-MHz B-scan image of the liver for guidance. Then the color Doppler mode was turned on to scan the sample to produce a crawling wave movie. A single frame of the crawling wave movie is shown in Figure 4. Multiple frames (at least 100 frames; the maximum number of frames that can be saved depends on the color flow region of interest size) were acquired for each crawling wave movie using the GE LOGIQ E9 system.

To generate the slowly moving interference patterns, the sources were driven by harmonic signals,  $f_1$  and  $f_2$ , with a slight difference between the vibration frequencies such that  $\Delta f \ll f$ , where  $\Delta f = |f_2 - f_1|$ . The estimated shear speed,  $c_s$ , was calculated from the Doppler cine video using the relationship:

$$(1) \quad c_s = 2 \frac{f}{\Delta f} \times \frac{dx}{dt},$$

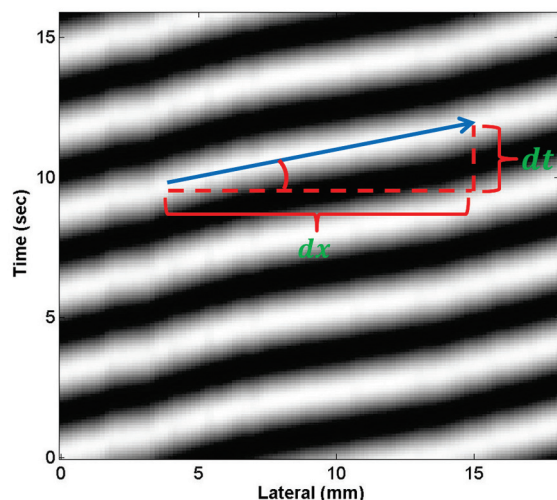
where the derivative  $dx/dt$  is extracted from the motion video. A time versus lateral distance image from 100-Hz crawling wave data is shown in Figure 5. Refer to Barry et al<sup>27</sup> for further descriptions of phantom preparation, the crawling wave setup and procedure, and the estimation algorithm.

**Figure 4.** Single crawling wave movie frame of a lean rat liver captured at a vibration frequency of 100 Hz.



Crawling wave experiments and subsequent shear speed estimations were performed for each liver sample using multiple discrete frequencies in the range of 60 to 260 Hz with frequency shifts of 0.35 Hz (eg,  $f_1 = 60$  Hz and  $f_2 = 60.35$  Hz,  $f_1 = 80$  Hz and  $f_2 = 80.35$  Hz, and so on). The crawling wave frequency range was appropriately chosen to increase the signal-to-noise ratio and reduce the reflections of the propagating shear waves at boundaries.

**Figure 5.** Motion slice extracted from 100-Hz crawling wave data. The angle of the motion stripes is indicative of the shear wave speed of the medium.



The raw data for each group consisted of shear wave speed estimates at 8 discrete frequencies between 60 and 260 Hz. These data were fit to a linear regression to obtain the slope (dispersion in meters per second per 100 Hz) and a reference value at 150 Hz, which was near the center of our measurement bandwidth. The limited size of each liver and limited frequency range studied make the dispersion (slope) calculation of each aggregated group more robust than taking slopes of each individual liver measurement.

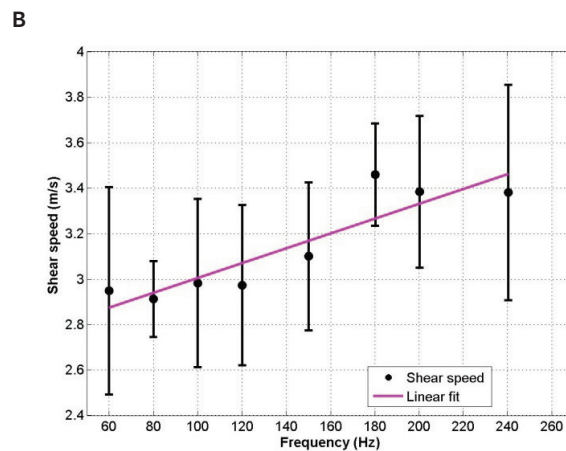
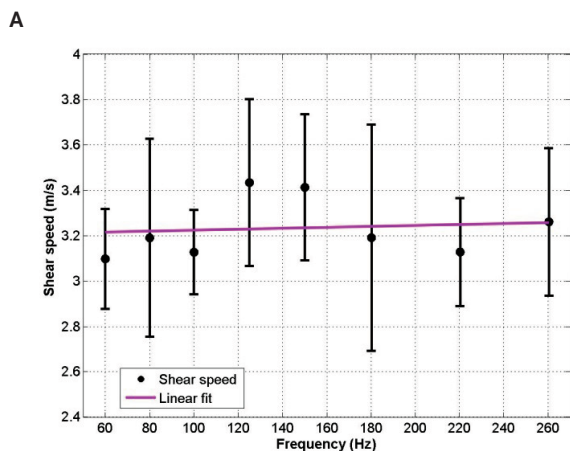
On completion of the shear speed estimations and TG measurements for all liver samples, the data were organized with respect to the fat concentration for analysis as a group.

## Results

The results of this study (Figure 6) found a very low dispersion (slope) of 0.02 m/s per 100 Hz in the lean group but a dispersion (slope) of 0.33 m/s per 100 Hz of shear wave bandwidth in the steatotic group over a range of crawling waves spanning from 60 to 260 Hz. Thus, dispersion was found to increase with steatosis in the rat liver model, whereas the shear speed at 150 Hz decreased slightly (Figure 7).

Histologic examination showed no macrosteatosis and less than 1% microsteatosis in the lean group and 5% macrosteatosis and 15% microsteatosis in the fatty liver group (Figure 8). The TG level for the lean rat livers was less than 5 mg/g, whereas fat livers had TG levels of 16 to 25 mg/g.

**Figure 6.** Shear speed versus frequency for lean (A) and fatty (B) groups showing higher dispersion in the fatty livers. The slope for the lean group is 0.02 m/s per 100 Hz; the slope for the fatty group is 0.33 m/s per 100 Hz. The lean group had TG levels of less than 5 mg/g. The fatty group had TG levels in the range of 16 to 25 mg/g.



## Discussion

The measurement of dispersion in human livers could be a useful assessment of steatosis, but some technical challenges remain. One is the need for accuracy in measuring the dispersion of the shear wave speed or attenuation within a limited bandwidth in vivo. Our studies to date demonstrate that in small leptin-deficient animal models,

**Figure 7.** Ninety percent confidence interval range for the linear fit of shear wave speed dispersion for lean and steatotic livers. Shown are the group analyses of 5 obese rats with average 5% macrosteatosis and 15% microsteatosis (red) and 5 lean control rats (blue). Increased dispersion and decreased shear speed is shown in the fatty liver group.

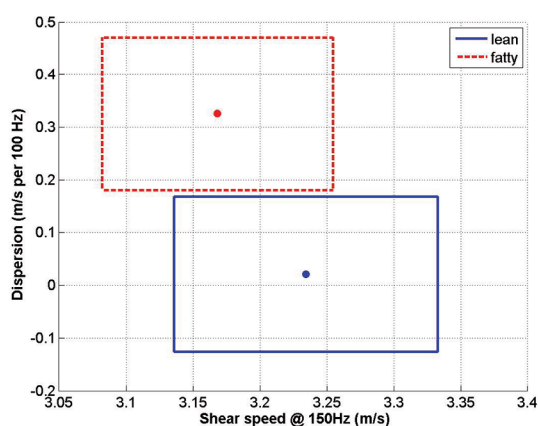
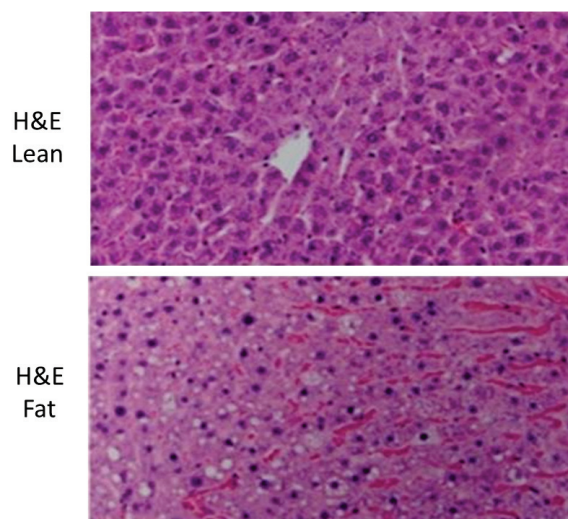


**Figure 8.** Representative histologic specimens from lean and steatotic livers at  $\times 700$  magnification. Fat-filled vacuoles appear as small clear voids in the bottom specimen. The fatty group averaged 5% macrosteatosis and 15% microsteatosis, indicating a relatively early stage of simple steatosis. H&E indicates hematoxylin-eosin.



the liver dispersion ranges from near 0 in lean livers to 0.4 m/s per 100 Hz in highly steatotic livers.<sup>24,27</sup> These findings mean, for example, that a steatotic liver shear speed of 2.0 m/s at 100 Hz will rise to 2.4 m/s at 200 Hz. The challenge lies in measuring this modest slope with high confidence over a limited region in the liver and in the presence of noise and physiologic motion. Furthermore, for assessment of early-stage steatosis, the dispersion increase (above the expected value for lean livers) will be even smaller, requiring more stringent accuracy and precision. Additionally, the combined effects of steatosis plus fibrosis in the liver will require additional studies. The use of crawling waves in vivo through the abdominal wall will require a modification to the techniques used in this study; one potential approach is detailed in a recent article.<sup>26</sup>

Some limitations of this study included the limited sample size ( $n = 5$  per group) and the presence of occasional shear wave artifacts likely caused by reflections at the liver-gelatin boundaries and the gelatin-air boundary at the edges of the prepared samples. Furthermore, the limited regions of interest in each liver and limited bandwidth of the crawling waves led us to analysis of the groups (lean versus steatotic) to attain reasonable confidence limits on the estimates of dispersion. The issue of how precise the dispersion measurement can be on an individual human liver in vivo remains for further research. Nonetheless, these results and those of previous studies on mice support the potential for use of shear wave dispersion for assessment of steatosis.

In conclusion, we have confirmed in 3 separate studies the validity of our dispersion hypothesis in animal models.

## References

1. Angulo P. Nonalcoholic fatty liver disease. *N Engl J Med* 2002; 346:1221–1231.
2. Lam B, Younossi ZM. Treatment options for nonalcoholic fatty liver disease. *Therap Adv Gastroenterol* 2010; 3:121–137.
3. Schreuder TC, Verwer BJ, van Nieuwkerk CM, Mulder CJ. Nonalcoholic fatty liver disease: an overview of current insights in pathogenesis, diagnosis and treatment. *World J Gastroenterol* 2008; 14:2474–2486.
4. Wanless IR, Lentz JS. Fatty liver hepatitis (steatohepatitis) and obesity: an autopsy study with analysis of risk factors. *Hepatology* 1990; 12:1106–1110.
5. Schuppan D, Schattenberg JM. Non-alcoholic steatohepatitis: pathogenesis and novel therapeutic approaches. *J Gastroenterol Hepatol* 2013; 28(suppl 1):68–76.
6. Williams CD, Stengel J, Asike MI, et al. Prevalence of nonalcoholic fatty liver disease and nonalcoholic steatohepatitis among a largely middle-aged population utilizing ultrasound and liver biopsy: a prospective study. *Gastroenterology* 2011; 140:124–131.

7. Ong JP, Pitts A, Younossi ZM. Increased overall mortality and liver-related mortality in non-alcoholic fatty liver disease. *J Hepatol* 2008; 49:608–612.
8. Bavu E, Gennisson JL, Couade M, et al. Noninvasive in vivo liver fibrosis evaluation using supersonic shear imaging: a clinical study on 113 hepatitis C virus patients. *Ultrasound Med Biol* 2011; 37:1361–1373.
9. Muller M, Gennisson JL, Defieux T, Tanter M, Fink M. Quantitative viscoelasticity mapping of human liver using supersonic shear imaging: preliminary in vivo feasibility study. *Ultrasound Med Biol* 2009; 35:219–229.
10. Boursier J, Isselin G, Fouchard-Hubert I, et al. Acoustic radiation force impulse: a new ultrasonographic technology for the widespread noninvasive diagnosis of liver fibrosis. *Eur J Gastroenterol Hepatol* 2010; 22:1074–1084.
11. Yin M, Talwalkar JA, Glaser KJ, et al. Assessment of hepatic fibrosis with magnetic resonance elastography. *Clin Gastroenterol Hepatol* 2007; 5:1207–1213.
12. Huwart L, Sempoux C, Vicaut E, et al. Magnetic resonance elastography for the noninvasive staging of liver fibrosis. *Gastroenterology* 2008; 135:32–40.
13. Palmeri ML, Wang MH, Dahl JJ, Frinkley KD, Nightingale KR. Quantifying hepatic shear modulus in vivo using acoustic radiation force. *Ultrasound Med Biol* 2008; 34:546–558.
14. Poynard T, Mathurin P, Lai CL, et al. A comparison of fibrosis progression in chronic liver diseases. *J Hepatol* 2003; 38:257–265.
15. Ferraioli G, Tinelli C, Dal Bello B, et al. Accuracy of real-time shear wave elastography for assessing liver fibrosis in chronic hepatitis C: a pilot study. *Hepatology* 2012; 56:2125–2133.
16. Wong VW, Vergniol J, Wong GLH, et al. Liver stiffness measurement using XL probe in patients with nonalcoholic fatty liver disease. *Am J Gastroenterol* 2012; 107:1862–1871.
17. Asbach P, Klatt D, Hamhaber U, et al. Assessment of liver viscoelasticity using multifrequency MR elastography. *Magn Reson Med* 2008; 60:373–379.
18. Friedrich-Rust M, Wunder K, Kriener S, et al. Liver fibrosis in viral hepatitis: noninvasive assessment with acoustic radiation force impulse imaging versus transient elastography. *Radiology* 2009; 252:595–604.
19. Huwart L, Sempoux C, Salameh N, et al. Liver fibrosis: noninvasive assessment with MR elastography versus aspartate aminotransferase-to-platelet ratio index. *Radiology* 2007; 245:458–466.
20. Klatt D, Hamhaber U, Asbach P, Braun J, Sack I. Noninvasive assessment of the rheological behavior of human organs using multifrequency MR elastography: a study of brain and liver viscoelasticity. *Phys Med Biol* 2007; 52:7281–7294.
21. Salameh N, Larrat B, Abarca-Quinones J, et al. Early detection of steatohepatitis in fatty rat liver by using MR elastography. *Radiology* 2009; 253:90–97.
22. Salameh N, Peeters F, Sinkus R, et al. Hepatic viscoelastic parameters measured with MR elastography: correlations with quantitative analysis of liver fibrosis in the rat. *J Magn Reson Imaging* 2007; 26:956–962.
23. Hoyt K, Castaneda B, Parker KJ. Two-dimensional sonoelastographic shear velocity imaging. *Ultrasound Med Biol* 2008; 34:276–288.
24. Barry CT, Mills B, Hah Z, et al. Shear wave dispersion measures liver steatosis. *Ultrasound Med Biol* 2012; 38:175–182.
25. Hah Z, Hazard C, Mills B, Barry C, Rubens D, Parker K. Integration of crawling waves in an ultrasound imaging system, part 2: signal processing and applications. *Ultrasound Med Biol* 2012; 38:312–323.
26. Partin A, Hah Z, Barry CT, Rubens DJ, Parker KJ. Elasticity estimates from images of crawling waves generated by miniature surface sources. *Ultrasound Med Biol* 2014; 40:685–694.
27. Barry CT, Hah Z, Partin A, et al. Mouse liver dispersion for the diagnosis of early-stage fatty liver disease: a 70-sample study. *Ultrasound Med Biol* 2014; 40:704–713.
28. Klain J, Fraser D, Goldstein J, et al. Liver histology abnormalities in the morbidly obese. *Hepatology* 1989; 10:873–876.
29. Levene AP, Kudo H, Armstrong MJ, et al. Quantifying hepatic steatosis: more than meets the eye. *Histopathology* 2012; 60:971–981.
30. Burant CF, Sreenan S, Hirano KI, et al. Troglitazone action is independent of adipose tissue. *J Clin Invest* 1997; 100:2900–2908.
31. Taylor LS, Porter BC, Rubens DJ, Parker KJ. Three-dimensional sonoelastography: principles and practices. *Phys Med Biol* 2000; 45:1477–1494.